Cancer Letters 449 (2019) 87–98

Contents lists available at ScienceDirect

Cancer Letters

journal homepage: www.elsevier.com/locate/canlet

Original Articles

Anti-tumor activity of antibody drug conjugate targeting aspartate-β-hydroxylase in pancreatic ductal adenocarcinoma

Katsuya Nagaoka[a,1], Xuewei Bai[a,b,1], Kosuke Ogawa[a], Xiaoqun Dong[a,c], Songhua Zhang[a], Yanmei Zhou[a,d], Rolf I. Carlson[a], Zhi-Gang Jiang[e], Steve Fuller[e], Michael S. Lebowitz[e], Hossein Ghanbari[e], Jack R. Wands[a,*]

[a] Liver Research Center, Rhode Island Hospital, Warren Alpert Medical School, Brown University, Providence, RI, USA
[b] Department of Pancreatic and Biliary Surgery, The First Affiliated Hospital of Harbin Medical University, Harbin, 150081, Heilongjiang Province, PR China
[c] Department of Internal Medicine, College of Medicine, The University of Oklahoma Health Sciences Center, Oklahoma City, OK, USA
[d] Department of Anesthesiology, The First Affiliated Hospital of Harbin Medical University, Harbin, 150001, Heilongjiang Province, PR China
[e] Sensei Biotherapeutics, Gaithersburg, MD, USA

ARTICLE INFO

Keywords:
Pancreatic cancer
Pulmonary metastasis
Cytotoxicity
ADC
ASPH

ABSTRACT

Pancreatic ductal adenocarcinoma (PDAC) is an extremely aggressive malignancy with very limited treatment options. Antibody drug conjugates (ADCs) are promising cytotoxic agents capable of highly selective delivery. Aspartate-β-hydroxylase (ASPH) is a type II transmembrane protein highly expressed in PDACs (97.1%) but not normal pancreas. We investigated anti-tumor effects of an ADC guided by a human monoclonal antibody (SNS-622) against ASPH in human PDAC cell lines and derived subcutaneous (s.c.) xenograft as well as a patient-derived xenograft (PDX) murine model with spontaneous pulmonary metastasis. The cytotoxic effects exhibited by several candidate payloads linked to SNS-622 antibody targeting ASPH$^+$ PDACs were analyzed. After *i.v.* administration of SNS-622-emtansine (DM1) ADC, the primary PDAC tumor growth and progression (number and size of pulmonary metastases) were determined. The PDAC cell lines, s.c. and PDX tumors treated with ADC were tested for cell proliferation, cytotoxicity and apoptosis by MTS and immunohistochemistry (IHC) assays. SNS-622-DM1 construct has demonstrated optimal anti-tumor effects *in vitro*. In the PDX model of human PDAC, SNS-622-DM1 ADC exerted substantially inhibitory effects on tumor growth and pulmonary metastasis through attenuating proliferation and promoting apoptosis.

1. Introduction

Pancreatic ductal adenocarcinoma (PDAC) is one of the most aggressive malignancies. Approximately, 80–85% of PDAC patients present with unresectable tumors at the time of diagnosis and over 90% of patients do not survive longer than 5 years with this malignancy [1,2]. Despite efforts in the development of surgery, chemoradiotherapy and immunotherapy, pharmacologic treatment of PDAC has remained challenging with very limited options. Therefore, it is essential to explore new strategies including targeted drugs for individuals with unresectable PDAC.

Antibody drug conjugates (ADC) are primarily designed to deliver a potent cytotoxic agent with high selectivity into tumor cells using an antibody directed against a specific antigen on the surface of tumor cells. Upon binding, the ADC is rapidly internalized, as a key determinate of anti-cancer efficacy [3]. Aspartate-β-hydroxylase (ASPH) is a type II transmembrane protein highly expressed in PDACs. We have previously reported robust ASPH protein expression in 101 of 104 PDACs (97.1%) using tissue microarrays, whereas no immunoreactivity in pancreatitis, normal pancreas, normal intestine or pancreatic neuroendocrine tumor [4]. In this study, we describe the development, evaluation and implementation of a novel ADC containing a cytotoxic payload as a potential therapeutic agent for ASPH positive PDACs and distant pulmonary metastatic spread.

* Corresponding author. Liver Research Center, Rhode Island Hospital and The Warren Alpert Medical School of Brown University, 55 Claverick Street, 4th Fl, Providence, RI, 02903, USA.
E-mail address: jack_wands_md@brown.edu (J.R. Wands).
[1] These authors contributed equally to this work.

https://doi.org/10.1016/j.canlet.2019.02.006
Received 17 September 2018; Received in revised form 31 January 2019; Accepted 5 February 2019

Abbreviations

ADC	antibody drug conjugate
ASPH	aspartate-β-hydroxylase
DMEM	Dulbecco's Modified Eagle's Medium
DM1	N_2'-deacetyl-N_2'-(3-mercapto-1-oxopropyl)-maytansine
DUO	duocarmycin
EGF	epidermal growth factor
FFPE	formalin-fixed paraffin embedded
H&E	hematoxylin and eosin stain
IACUC	Institutional Animal Care and Use Committee
IHC	immunohistochemistry
I.V.	intravenous
MAB	monoclonal antibody
MMAE	monomethyl auristatin E
NSG	NOD scid gamma
PDAC	pancreatic ductular adenocarcinoma
PDX	patient-derived xenograft
T-DM1	ado-trastuzumab emtansine

2. Materials and methods

2.1. Cell lines

The human pancreatic cancer cell lines AsPC-1 and MIA PaCa2 were purchased from the American Type Culture Collection. Cells were cultured at 37 °C in a humidified atmosphere containing 5% CO_2 in corresponding medium supplemented with 10% fetal bovine serum and penicillin-streptomycin. The culture medium used was RPMI 1640 for AsPC-1, and high-glucose (25 mM D-glucose) Dulbecco's Modified Eagle's Medium (DMEM) for MIA PaCa2 cells, respectively. We have established a stable MIA PaCa2 cell line overexpressing ASPH by using the lentiviral transfection system [4,5].

2.2. Antibody

The anti-ASPH human antibody "622" was generated as described previously [6]. The murine monoclonal antibody (FB50) was developed in our laboratory [7]. Anti-Phospho-Histone H3 (Ser10) (#9701), and anti-Cleaved Caspase-3 (Asp175) (#9661) antibodies were purchased from Cell Signaling Technology. Anti-Ki67 antibody (NCL-Ki67p) was purchased from Leica Biosystems. Anti-GAPDH antibody (sc-32233) was purchased from Santa Cruz Biotechnology. The TUNEL colorimetric IHC detection kit was obtained from ThermoFisher Scientific and performed according to manufacturer instructions.

2.3. Development of ADCs with cytotoxic payloads

SNS-622 was conjugated to one of the three different drugs: maytansinoid (DM1), monomethyl auristatin E (MMAE) or duocarmycin (DUO). DM1 was conjugated via a non-cleavable thioether linker maleimidocaproyl (MC), while MMAE or DUO were conjugated using valine-citruline (vc) containing linkers, which are cleavable by cathepsin B in the endosomal compartment (Table I supplemental information). DM1 was conjugated at a 10:1 M ratio with antibody while MMAE and DUO was conjugated at a drug-to-antibody ratio (DAR) of 5:1 and 2.2:1, respectively. Conjugation of drugs to the SNS-622 antibody had little effect on its affinity for antigen, ASPH. Drug-Linker payloads were purchased from Levena Biopharma (San Diego, CA). Conjugates were purified by dialysis using a 30 K Da MWCO Dialysis Device overnight in 1 × PBS (pH 7.4) with a total of three buffer changes.

ADCs were characterized by UV-vis, SDS-PAGE, HIC-HPLC and SEC-HPLC. DARs were determined by UV-vis & HIC-HPLC (Tables I and II; supplemental information). Binding affinities were determined by immunoassay on fixed cancer cells (H460, human lung cancer line): ~0.1, 0.2 and 0.5 nM for SNS-622-DM1, SNS-622-MMAE and SNS-622-DUO, respectively. The affinity of SNS-622 for ASPH as expressed on live cells has previously been shown to be ~1 nM.

2.4. Immunohistochemistry staining

Immunohistochemistry (IHC) staining was performed as previously described [4]. In brief, IHC was conducted on 4-μm thick formalin-fixed paraffin embedded (FFPE) unstained sections. After deparaffinization and antigen retrieval, endogenous peroxidase activity was quenched by a 30-min treatment with 3% hydrogen peroxide dissolved in methanol. The staining procedure was performed using the VECTASTAIN Elite ABC kit (PK-6101, PK-6102 and PK-6103 Vector Laboratories). Primary antibodies were incubated at 4 °C overnight. Color development was performed using DAB Peroxidase (HRP) substrate kit (SK-4100, Vector Laboratories). Subsequently, Hematoxylin staining was performed.

For quantitation of cell staining, 6 microscopic fields were randomly selected at 400 × . The total number of DAB positive staining cells including nuclear staining, were counted for each sample and the percentage of positive cells was calculated. For quantitation of the staining on tissue sections, immunostained slides were scanned at a magnification of 100 × , then DAB and Hematoxylin staining were evaluated using ImageJ software (U. S. National Institutes of Health, Bethesda, Maryland, USA, https://imagej.nih.gov/ij/), with plugin "Color Deconvolution" [8].

2.5. MTS assay

The cytotoxicity of each ADC was measured using an MTS assay kit containing a tetrazolium compound [3-(4,5-dimethylthiazol-2-yl)-5-(3-carboxymethoxyphenyl)-2-(4-sulfophenyl)-2H-tetrazolium, inner salt; MTS] (Promega #G3582). Cells were seeded on a 96-well plate at a density of 5,000 cells/well. Cells were incubated for 48 h with naked antibody or ADC, respectively. Naked antibody or ADC was sterilized through a 0.22 μm spin filter before use. To determine numbers of live cells, MTS solution was added to the incubation for the final 1 h and absorbance was measured in a microplate reader at a wavelength of 490 nm with a reference at 690 nm.

2.6. Western blots

Western blot analysis was performed as previously described [9]. In brief, cell lysates were separated by SDS-PAGE and transferred to PVDF membranes. Blots were incubated with each primary antibody overnight at 4 °C and then incubated with corresponding secondary antibodies for 1 h. Protein expression was visualized with enhanced chemiluminescence by ECL Western blotting system (SuperSignal West Pico Chemiluminescent Substrate; Thermo Scientific, Waltham, MA, USA).

2.7. Animal model

The orthotopic model using the MIA PaCa2 vector and ASPH high expressing cell lines were established as described [4]. We also established a patient-derived xenograft (PDX) murine model from patients undergoing surgical resection of PDAC at Rhode Island Hospital. The 5 to 6-week-old female NOD scid gamma (NSG) mice were employed. The surgically resected tumor tissue was diced into 5 × 5 × 5 mm^3 pieces. One piece of tumor tissue was subcutaneously transplanted into each mouse via a small incision in the lower back after anesthesia with isoflurane. An analgesic with Buprenorphine was injected for 3 days

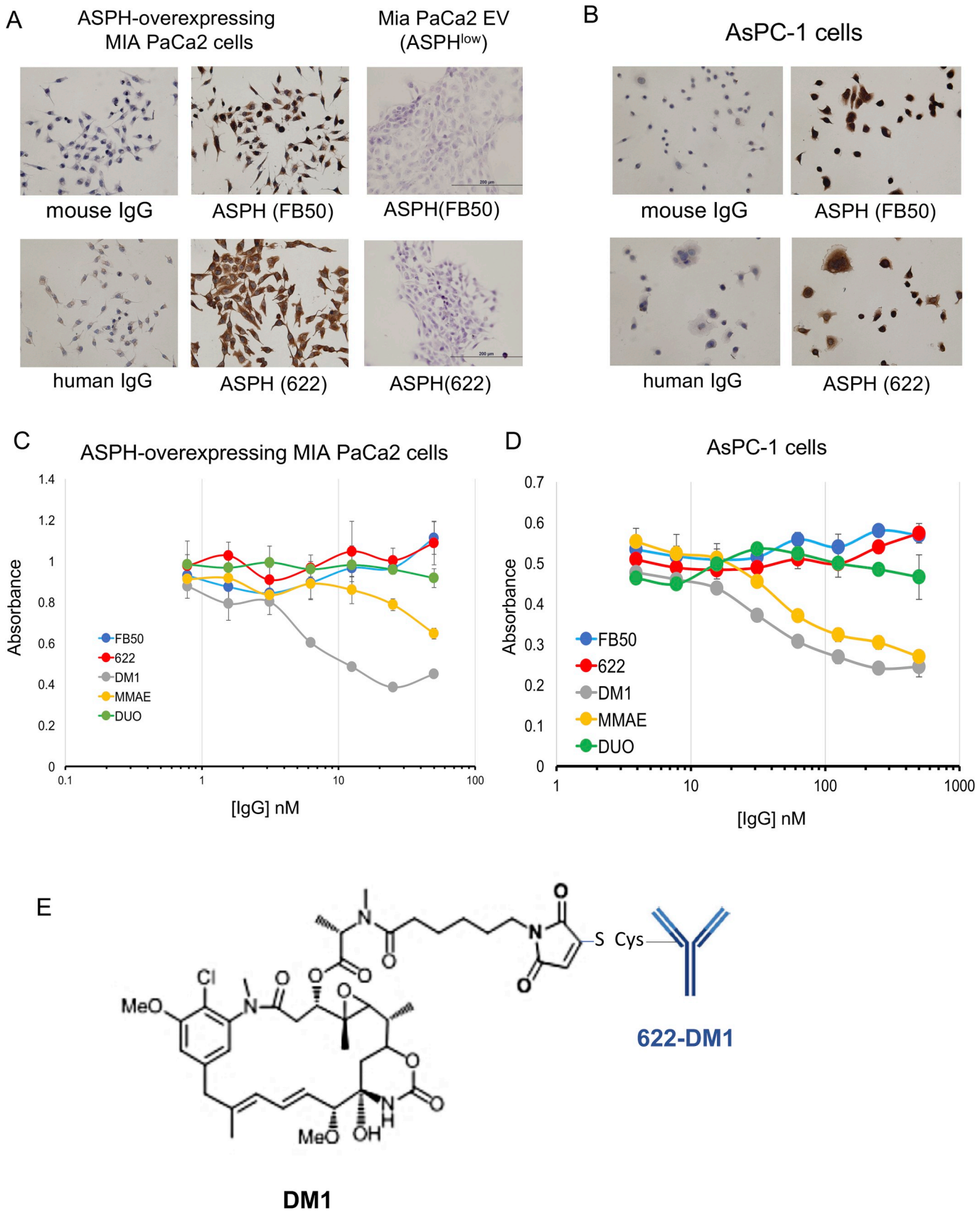

Fig. 1. Comparisons of anti-tumor effects generated by different ADCs in human PDAC cell lines. IHC staining using murine FB50 and human 622 antibodies against ASPH in (**A**) MIA PaCa2 cells with exogenous ASPH and (**B**) AsPC-1 cells with high endogenous ASPH. MTS assay was performed in (**C**) MIA PaCa2 and (**D**) AsPC-1 cells. These cell lines were incubated with different concentrations (range: 0–50 or 0–500 nM, respectively) of ADCs: 622-MMAE, 622-DUO, 622-DM1 and control unconjugated FB-50 and 622 mAbs for 48 h. The initial concentration of MIA PaCa2 and AsPC-1 plated cells in the MTT assay were the same in all groups. Values represented mean ± S.D. from experiments performed in triplicate. MMAE, monomethyl auristatin E; DUO, duocarmycin; DM1, emtansine. (**E**) Structure of SNS-622-DM1 conjugate.

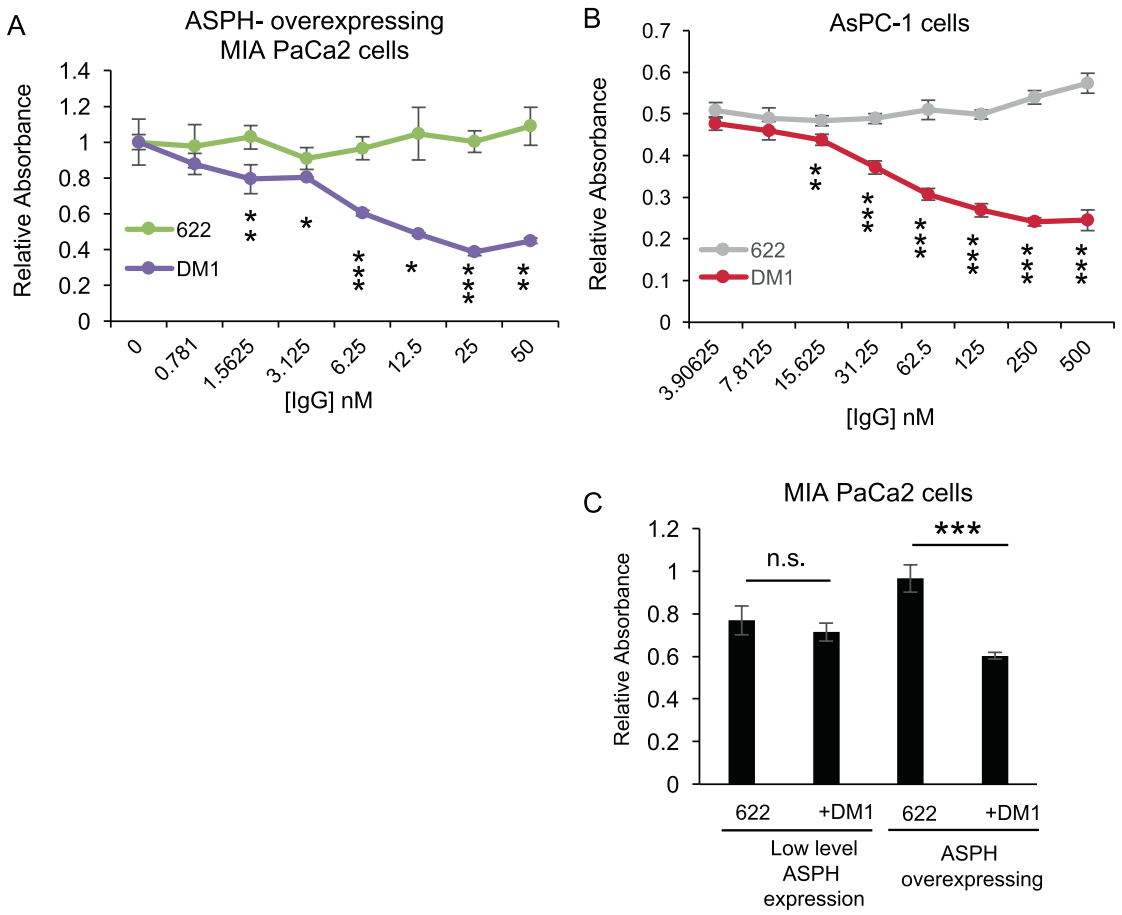

Fig. 2. The anti-ASPH antibody conjugated to DM1 selectively inhibits tumor cell viability *in vitro*. (A) MTS assay of ASPH overexpressing MIA PaCa2 cells treated with 0–50 [IgG] nM 622 mAb or SNS-622-DM1 for 48 h. **(B)** MTS assay of AsPC-1 cells treated with 0–500 [IgG] nM 622, or 622-DM1 for 48 h. **(C)** Inhibitory effects of 6.25 [IgG] nM 622 or 622-DM1 on cell viability in parental (empty vector transfected) vs. ASPH overexpressing MIA PaCa2 cells. Values represented the mean ± S.D. from triplicate samples. *P < 0.05, **P < 0.01, ***P < 0.005 versus the group treated with 622 mAb.

after surgery. The SNS-622 naked antibody or SNS-622-DM1 was administered by intravenous tail-vein injection. Body weight and tumor size were measured twice a week. Tumor volume was calculated using the modified ellipsoid formula (0.5 × length × width^2) [10,11]. Body weight was measured twice a week. After 5–8 weeks, the animals were euthanized. All lung tissues were immersed in Bouin's fixative solution (Sigma-Aldrich, HT10132) and metastatic nodules on the surface of the lungs were counted. Animal experiments were conducted in accordance with the guidelines of the Institutional Animal Care and Use Committee (IACUC) at Rhode Island Hospital.

2.8. Statistical analysis

All statistical analyses were performed using SPSS software (version 16.0). Differences between two groups were evaluated by student's t-tests unless otherwise stated. Equality of variance was examined using the f-test. A p value of < 0.05 (2-tailed) was considered statistically significant.

3. Results

3.1. Cytotoxicity on ASPH overexpressing PDAC cell lines exhibited by SNS-622 anti-ASPH antibody conjugates

The anti-tumor effects of SNS-622 conjugated to multiple cytotoxic payloads including MMAE, DUO, and DM1 on MIA PaCa2 (stably transfected and overexpressing ASPH) and AsPC-1 (with high endogenous expression of ASPH) cell lines were evaluated [4]. The IHC staining revealed ASPH was highly expressed in both cell lines and recognized by both murine (FB50) and human SNS-622 anti-ASPH antibodies (Fig. 1A and B).

A MTS assay was performed using the tetrazolium compound to evaluate cytotoxicity over a range of drug concentrations. Examples of positive and negative results among several candidate cytotoxic payloads delivered by SNS-622 are depicted in Fig. 1C and D. The highest activity was demonstrated with SNS-622-DM1, the structure of which is presented in Fig. 1E. This ADC construct inhibited PDAC cell proliferation and viability of MIA PaCa2-ASPH and AsPC-1 cell lines. The biologic activity of SNS-622-DM1 was observed at very low concentrations of 25–50 nM (IgG) as shown by a 60% reduction in proliferation. SNS-622-DM1 significantly attenuated cellular proliferation compared to SNS-622-antibody alone in MIA PaCa2 (Fig. 2A) and AsPC-1 cells (Fig. 2B). To examine the specificity of SNS-622-DM1 targeting ASPH-expressing cells, cytotoxicity was compared between empty vector and ASPH overexpressing MIA PaCa2 cells (Fig. 2C). Both cell lines were treated with very low concentrations of SNS-622 or SNS-622-DM1 at 6.25 nM (IgG) for 48 h. Inhibition of cell growth was observed in ASPH-overexpressing MIA PaCa2 cells treated with SNS-622-DM1 compared to SNS-622 alone. In contrast, such anti-tumor activity was not observed in empty vector transfected MIA PaCa2 cells with very low endogenous ASPH expression (Fig. 2C). These results suggest that SNS-622-DM1 is specific and a potent cytotoxic agent with anti-tumor effects on PDAC overexpressing ASPH.

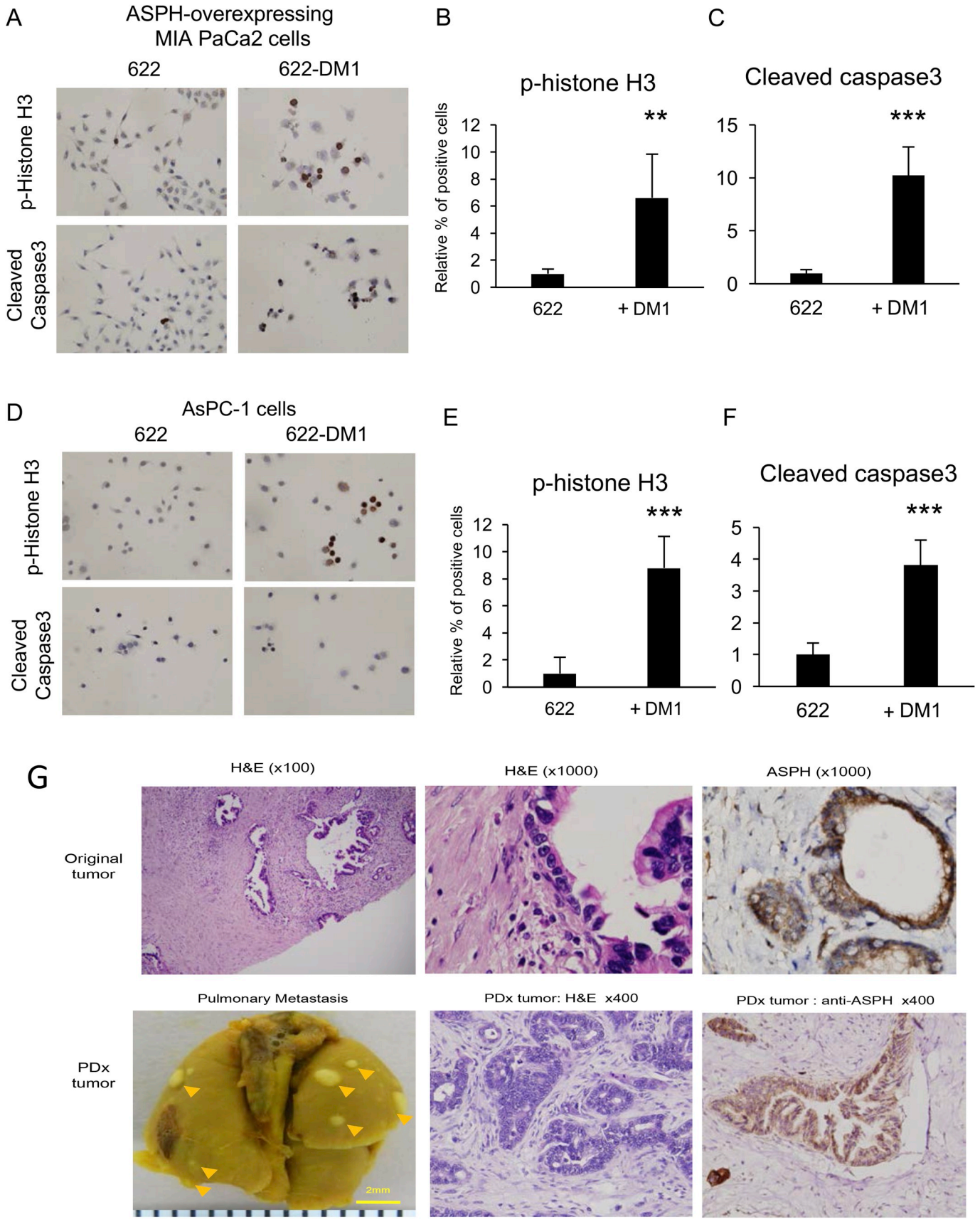

(caption on next page)

Fig. 3. PDAC cell lines treated with SNS-622 anti-ASPH conjugated to DM1 accumulates in the G2/M phase of cell cycle and exhibits apoptosis. (**A**) IHC staining to detect levels of p-Histone H3 and cleaved caspase 3 in ASPH overexpressing MIA PaCa2 cells. (**B**) Relative number of p-Histone H3 positive cells in panel (**A**). (**C**) Relative number of cleaved caspase 3 positive cells in panel (**A**). (**D**) IHC staining to detect levels of p-Histone H3 and cleaved caspase 3 in AsPC1 cells. (**E**) Relative number of p-Histone H3 positive cells in panel (**D**). (**F**) Relative number of cleaved caspase 3 positive cells in panel (**D**). Total number of positive cells with nuclear staining were counted and the percentage of positive cells determined. (**G**) Comparison of histologic features between the original tumor derived from PDAC patient (top panels) and the primary tumor derived from PDX model (bottom panels). Note that the dense stroma has been preserved in the PDX tumor as compared to the original human tumor. The pulmonary metastases in the NSG mice have recapitulated the patient's clinical course. Both the original human tumor and PDX primary/metastatic tumor (F2 generation) highly express ASPH as described by IHC. Values represent mean ± S.D. derived from six replicate samples. **P < 0.01, ***P < 0.005 versus the 622 mAb treatment group.

3.2. The SNS-622-DM1 ADC effects cell cycle progression and induces apoptosis in PDAC cells

To clarify the possible mechanisms underlying SNS-622-DM1 inhibitory effects on cell proliferation and viability, the expression levels of mitotic and apoptotic markers were examined in PDAC cell lines treated with SNS-622-DM1 for 48 h. The IHC analysis revealed significant accumulation of tumor cells in the G2/M phase of cell cycle as measured by phosphorylation of histone H3 at Serine 10 (p-histone H3). Prominent staining was observed in ASPH overexpressing MIA PaCa2 cells upon exposure to 10 nM of SNS-622-DM1 (Fig. 3A upper panel, B). Furthermore, SNS-622-DM1 treatment significantly increased the cellular level of cleaved caspase 3, the active form of this apoptosis-related protein, in PDAC cells compared to treatment with SNS-622 naked antibody (Fig. 3A lower panel, C). These results suggest that SNS-622-DM1 induced PDAC cell cycle arrest, which subsequently underwent apoptosis. Similarly, AsPC-1 cells with high endogenous expression of ASPH [4] treated with SNS-622-DM1 also demonstrated cell cycle arrest (Fig. 3D upper panel, E) and apoptosis (Fig. 3D lower panel, F). After performing the IHC staining, there was an initial separation of the color information acquired with DAB and hematoxylin staining using Image J software and its plugin “color deconvolution”. The number of IHC staining positive cells with DAB and the number of nuclei stained with hematoxylin for p-histone H3 and cleaved caspase 3 were calculated. Therefore, the cell numbers between 622-DM1 and the 622 groups were adjusted. We established a PDX model that exhibited spontaneous metastases from the primary human tumor grown on the back of NSG mice to the lung. This phenotype was observed in the tumor derived from the patient with PDAC as well (Fig. 3G).

3.3. Tumor growth inhibitory efficacy of SNS-622-DM1 ADC in a PDX model of human PDAC

In vitro studies have revealed that SNS-622 binds to ASPH on the surface of tumor cells and is internalized [6]. The efficacy of SNS-622-DM1 on PDAC primary tumor growth and metastasis was investigated. A novel PDX model of human PDAC was employed. Mice bearing an approximately 100 mm^3 tumor xenograft were intravenously injected weekly with 2.5 mg/kg of SNS-622 or SNS-622-DM1, and tumor growth was monitored. Primary PDAC tumor growth was significantly reduced by day 35 in response to ADC compared to SNS-622 naked antibody or non-treated control (Fig. 4A). The NSG mice received SNS-622-DM1 showed no adverse effects and maintained their body weight (Fig. 4B). It was confirmed that SNS-622-antibody and SNS-622-DM1 demonstrated strong binding to ASPH on cancer cells in the PDX model (Fig. 4D) in comparison with negative and positive controls (Fig. 4C). In addition, IHC analysis of the PDAC tumors of PDX mice using p-histone H3 staining, revealed that SNS-622-DM1 increased the number of tumor cells in the G2/M phase of the cell cycle. More importantly, SNS-622-DM1 treatment induced expression of cleaved caspase 3 (arrows) and TUNEL positive cells compared to treatment with SNS-622 naked antibody (Fig. 4D and E). These observations suggested that SNS-622-DM1 strongly bound to ASPH, inducing cell cycle arrest and promoting apoptosis as possible mechanisms for anti-tumor effects.

3.4. The SNS-622-DM1 ADC inhibits lung metastasis in a PDX model of PDAC

This PDX model was established from an individual with primary PDAC who had developed spontaneous lung metastasis during the clinical course. This phenotype was faithfully maintained in the PDX model. Serial passages of this PDAC tumor in NSG mice confirmed the durability and transmitability of this metastatic phenotype from the F2 to F9 generation, thus far. We evaluated the effects of SNS-622-DM1 administration on metastatic spread to the lungs. The NSG mice were treated with SNS-622 or SNS-622-DM1 using the protocol (dosing, route and interval of administration) as shown in Fig. 5A. The development and progression of metastatic nodules in the lungs after the treatment were assessed (Fig. 5B). After 6 weeks, the number of macro-metastatic nodules on the surface of lungs was determined. The mean number of nodules was 13.9 per animal in the untreated control group and 3.25 per animal in the SNS-622-DM1 treated group (P = 0.01, Fig. 5C and D). ASPH was substantially expressed in the lung metastatic nodules (Fig. 5E). Moreover, treatment with SNS-622-DM1 was associated with accumulation of p-histone H3 in the tumor nodules as revealed by IHC staining (Fig. 5E, yellow arrowheads).

3.5. Specificity of the ADC for ASPH expressing tumors

To demonstrate the specificity of the SNS-622 human anti-ASPH mAb for ASPH expressing PDACs, MIA PaCa2-empty vector and MIA-PaCa2-ASPH cell lines generated s.c. tumors in the NSG mice were treated with SNS-622-DM1 and a non-relevant IgG mAb also conjugated with DM1, respectively (Fig. 6A). Only MIA-PaCa2-ASPH (with high exogenous ASPH as shown in Fig. 6B) tumors treated with SNS-622-DM1 exhibited a reduced growth rate; whereas no anti-tumor effects of IgG-DM1 were noted (Fig. 6C). Fig. 6D demonstrates the expression levels of ASPH in the parental and overexpressing Mia PaCa2 cell lines derived from the control, IgG-DM1 and 622-DM1 treatment groups.

To confirm the specificity of SNS-622-DM1, the parental MIA PaCa2 cells with low endogenous ASPH generated tumors were established on the left shoulder while MIA PaCa2-ASPH generated tumors on the right shoulder of the same animal (Fig. 7A). The ADC, SNS-622-DM1, was administered at 2.5 mg/kg *i.v.* to 8 mice weekly (× 5). Compared to MIA PaCa2-empty vector generated tumors, MIA PaCa2-ASPH generated tumors were substantially inhibited in response to SNS-622-DM1 treatment (Fig. 7B). Consistent with *in vitro* results, caspase 3 cleavage was upregulated in the MIA PaCa2-ASPH derived tumors treated with SNS-622-DM1 (Fig. 7C). Direct comparisons of ASPH and p-histone H3 expression as well as apoptosis markers cleaved caspase-3 and TUNEL assays are shown in Fig. 7D. There were 12 animals in each group and treatment with SNS-622-DM1 was associated with cell cycle arrest and increased apoptosis in high and low expressing ASPH Mia PaCa2 cells.

4. Discussion

Several ADCs under clinical investigation have demonstrated cytotoxicity on cancer cells through disrupting functions, structures or dynamics of tubulins. Recently, US FDA has approved tubulin inhibitor-based ADCs, brentuximab vedotin for the treatment of Hodgkin's lymphoma and anaplastic large cell lymphoma [12]. Another tubulin

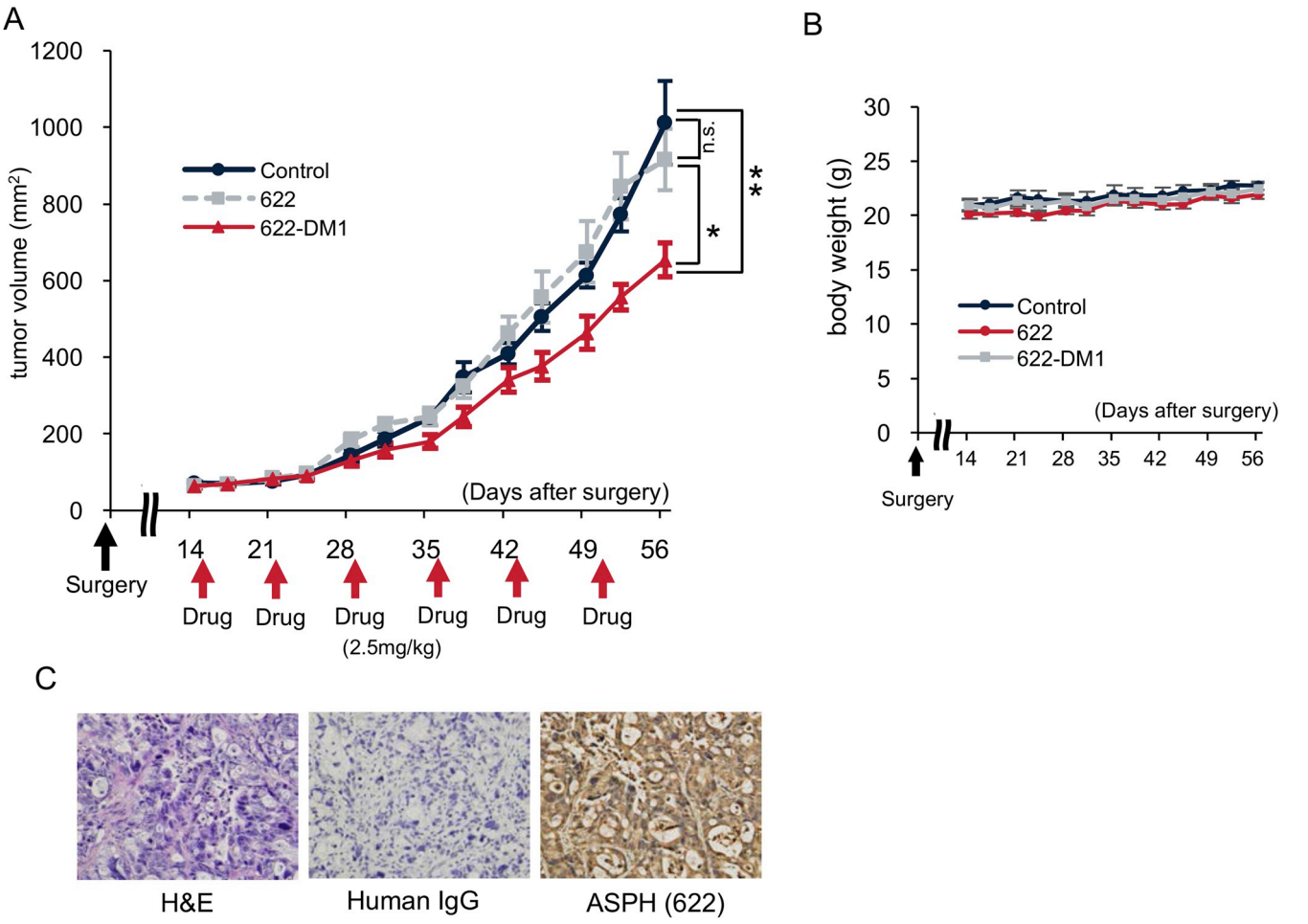

(caption on next page)

Fig. 4. Antibody conjugated DM1 demonstrates anti-tumor effects in PDX model of PDAC. (**A**) Mice xenografted human PDAC were treated once a week with 622 naked mAb or 622-DM1 (2.5 mg/kg) through injection into the tail vein. Values represent mean ± S.E.M. derived from each group (SNS-622, n = 8; SNS-622-DM1, n = 8; untreated control, n = 5). *P < 0.05, **P < 0.01, versus 622 or untreated control group. (**B**) Body weight of tumor-bearing mice in each group during the treatment. Values represent mean ± S.E.M. (**C**) Representative example of H&E and IHC staining on subcutaneous xenografts in untreated control at 400 × magnification. IHC was performed using a human non-relevant IgG (1 mg/ml, 1:1,000) or 622 mAb (1 mg/ml, 1:1,000). (**D**) Representative examples of IHC image at 400x magnification using the anti-ASPH murine FB50 mAb, or antibodies against mitotic marker p-histone H3 and apoptosis marker cleaved caspase 3 and the TUNEL staining on the subcutaneous human PDAC xenografts of each group treated with SNS-622 or SNS-622-DM1. (**E**) Quantitative analysis of panel (**D**). Values represent the mean ± S.D. derived from six different tumors. *P < 0.05, **P < 0.01 versus the treatment group with SNS-622 antibody.

inhibitor-based ADC, ado-trastuzumab emtansine (T-DM1) was approved as the first ADC therapeutic agent to treat human epidermal growth factor 2 (HER2)-positive breast cancer [13,14]. Brentuximab vedotin contains monomethyl auristatin E (MMAE) as a cytotoxic payload, while T-DM1 uses emtansine (DM1) as a payload. Both MMAE and DM1 inhibit tubulin function, resulting in cell cycle arrest in the G2/M phase and induction of apoptosis [15]. However, no ADCs have been approved by FDA for pancreatic cancer and very a few targeted antigens have been explored for construction of such ADCs [3,16].

We have recently identified and characterized ASPH as a target antigen on the surface of PDAC tumor cells. As a member of α-ketoglutarate dependent dioxygenase family [17,18], ASPH catalyzes the hydroxylation of aspartyl and asparaginyl residues in epidermal growth factor (EGF) like repeats of various proteins for signal transduction, including Notch receptors and ligands. The ASPH is conserved in mammalian evolution and the human protein sequence is 85% identical to rats and mice respectively; the catalytic site in the C-terminal region is 100% conserved among the three species. As an oncofetal protein expressed in embryonic development, it is “shut off” at birth, only to re-emerge during oncogenesis. Therefore, ASPH is proposed to generate and maintain malignant phenotypes in cancer, such as PDAC [4,17,18]. Overexpression of ASPH stimulates PDAC cell proliferation, migration, invasion, metastases and anchorage independent growth. Knockdown with shRNAs, knockout with CRISPR-Cas9 or inhibition of enzymatic activity with a site directed mutation in the catalytic site (H675Q) and a small molecule inhibitor (SMI) could impair ASPH-mediated malignant phenotype [4].

Immunohistochemical staining for protein expression and RT-PCR for mRNA upregulation have revealed that approximately 85% of hepatitis C virus (HCV) and hepatitis B virus (HBV) related HCC, as well as 95% of cholangiocarcinoma's exhibit upregulation of the ASPH gene [17–22]. It is overexpressed in 97.190 of PDAC's [4]. High expression confers a poor prognosis characterized by early disease reoccurrence, reduced overall survival and a highly undifferentiated aggressive phenotype [23,24].

The known mechanism(s) underlying ASPH's transforming activity in PDAC are the following. ASPH overexpression activates Notch1 signaling and upregulates downstream genes responsible for cell proliferation, migration, invasion and metastasis. ASPH binds directly to Notch1 receptor followed by generation of the ICD (intracellular domain) which translocates to the nucleus of PDAC cells and thus acts as a transcriptional factor. Transcriptional activation of ASPH is accomplished through well-known upstream growth factor signaling pathways. Thus, this molecule links upstream growth factor signaling to downstream Notch1 activation in tumorigenesis [18,20]. Recently, we have found other potential mechanisms responsible, in part, for its oncogenic properties by inhibiting apoptosis and enhancing cancer stem cell formation in PDAC [4]. This enzyme may regulate cell cycle control through phosphorylation of RB and impairs cell senescence [20]. Therefore, as a fundamental factor, the upregulation of ASPH contributes to PDAC oncogenesis.

It is noteworthy that several ADCs are undergoing clinical trials for PDAC. For example, TAK-264 (MLN0264) contains MMAE conjugated to anti-guanylyl cyclase C antibody. A phase II study on TAK-264 against PDAC is in progress [25,26]. Preclinical studies have been performed for PDAC and prostate cancer using another ADC, ASG-5ME [27]. The ASG-5ME contains MMAE conjugated to anti-SLC44A4 antibody. For breast cancer patients, T-DM1 exerts an antitumor effect by binding to HER2 protein [28]. Further attention has been paid to T-DM1 for treating different types of cancer, such as Her2 overexpressing gastric cancer [29,30] and colorectal cancer [31]. The proportion of Her2 positivity in PDAC has been reported to be 21%–45% [28,32,33], and clinical trials using T-DM1 on Her2 positive PDAC may be forthcoming.

It has been challenging to develop and evaluate efficient drugs that inhibit metastatic spread, due to lack of suitable animal models that realistically recapitulate histology and pathology of human tumors. We describe here a novel PDX derived from a patient with primary PDAC and subsequent pulmonary metastasis. In this corresponding PDX model, metastases to the murine lungs were spontaneously developed from a subcutaneous grown neoplasm on the back of NSG mice. It has been hypothesized that ASPH functions as a driver of pulmonary metastasis, partially attributable to Notch signaling activation [7,24,34–40].

A major challenge for drug delivery in PDAC treatment is desmoplasia (extremely dense stroma surrounding the tumor cells). This phenotype was recapitulated vividly in the PDX model. Desmoplasia significantly limits the access of ADCs to PDAC tumor cells. More profound inhibition of primary tumor growth was achieved in MIA PaCa2-ASPH by SNS-622-DM1, which is a clonal derived tumor without dense stroma. Notably, this ADC also exerted substantial inhibitory effects on the formation, growth and progression of pulmonary metastasis in the PDX model. The tumor tissue was derived from a patient who had pulmonary involvement during tumor progression.

The SNS-622-DM1 ADC demonstrated specificity for ASPH with respect to an ADC based on DM1 conjugated to a non-relevant IgG1 (Fig. 6). This ADC was highly active in tumors derived from MIA PaCa2 cells with robust exogenous expression of ASPH compared to the parenteral cells (Fig. 7), where there was little, if any, reduction in tumor development, growth and progression. Collectively, the novel ADC, SNS-622-DM1, has therapeutic potential in a murine PDX model for human PDAC and xenografted PDAC tumors generated by MIA PaCa2 cells overexpressing ASPH. This ADC inhibits the growth of primary tumor and metastatic spread to the lung. Mechanistically, SNS-622-DM1 is effective in inducing cell cycle arrest and promoting apoptosis of PDAC cells. Therefore, SNS-622-DM1 is a promising therapeutic agent to target ASPH in patients with PDAC and progressive development of a metastatic burden before and after surgical resection of the primary tumor.

Author contributions

Study concept and design: K.N., H.G., X.D., J.W.

Acquisition of data: K.N., X.B., S.Z., R.C., Y.Z.

Analysis and interpretation of data: K.N., S.F., Z-G.J., M.L., H.G., J.W.

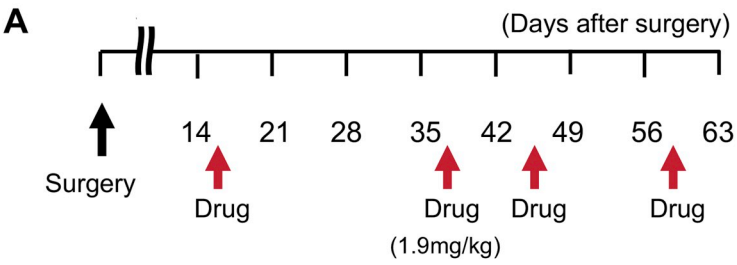

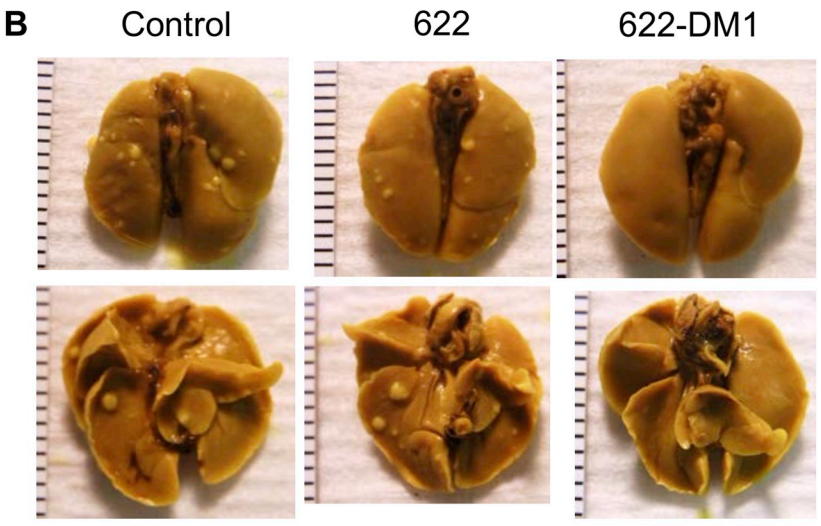

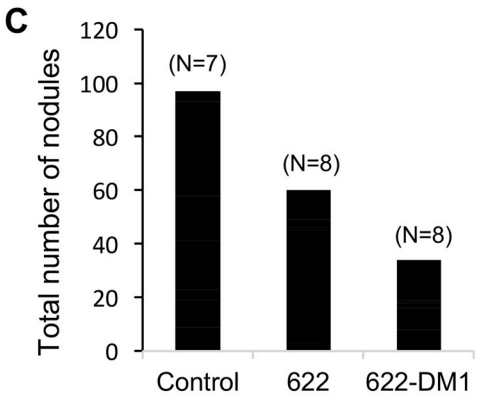

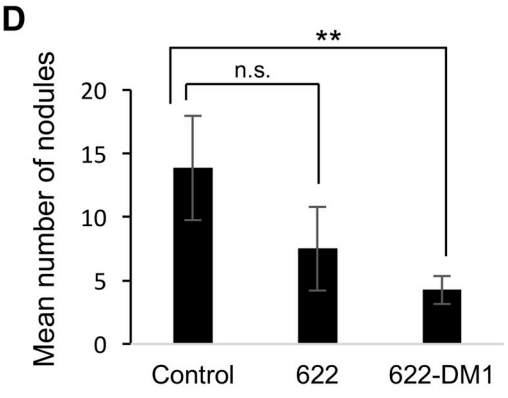

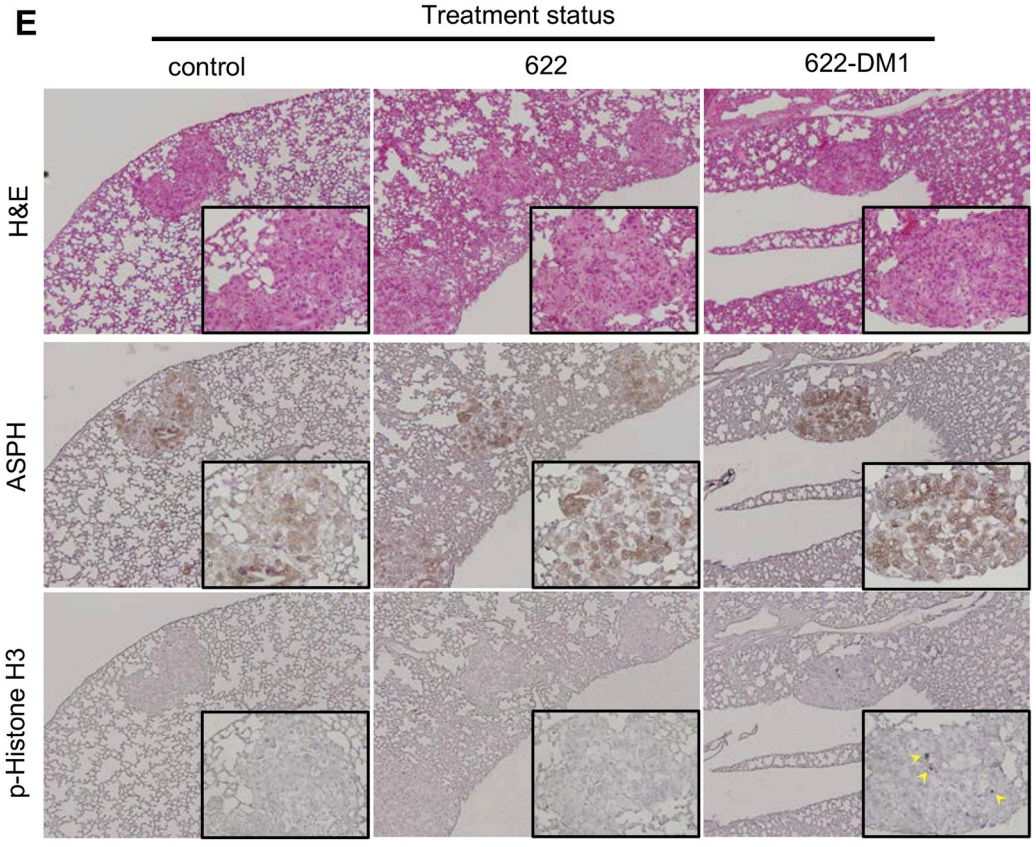

(caption on next page)

Fig. 5. The SNS-622-DM1 conjugate suppresses lung metastases in a PDX model of PDAC derived from a patient with spontaneous pulmonary metastasis. (**A**) Schedule of treatment with SNS-622 or SNS-622-DM1. Mice were injected with SNS-622 antibody or SNS-622-DM1 (1.9 mg/kg) via tail-vein. (**B**) Macroscopic view of the lung in the PDX model demonstrating pulmonary metastases. This indicates the phenotype of the PDX primary tumor is maintained in the NSG mice. (**C**) Total number of metastatic nodules in each group after fixation in Bouin's solution. (**D**) The mean number of metastatic nodules in each group. Values represent mean ± S.E.M. derived from pulmonary spread per group (untreated control, n = 7; SNS-622, n = 8; SNS-622-DM1, n = 8). Difference between two groups was evaluated by Mann-Whitney *U* test. (**E**) Histologic and IHC staining images of metastatic nodules in the lung in the PDX model. (100 × and 400 × magnification for H &E and IHC staining using anti-ASPH FB50 mAb, or anti-p-histone H3 antibody). Increased p-histone H3 accumulation was observed prominently in the SNS-622-DM1 treatment group (yellow arrowheads).

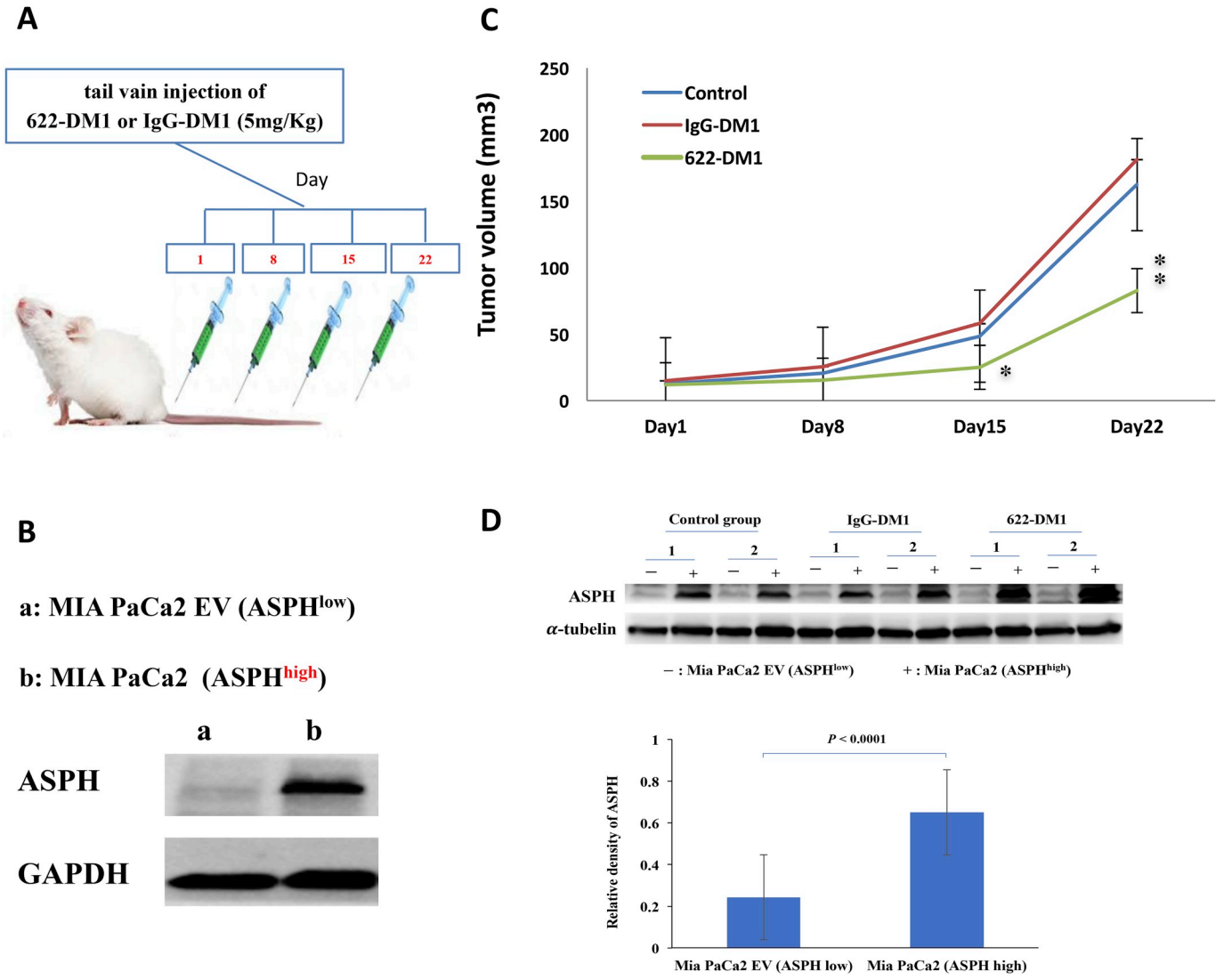

Fig. 6. Effects of SNS-622-DM1 on tumors generated by ASPH overexpressing MIA PaCa2 cell line. (**A**) Experimental design for s.c. murine model. (**B**) Expression of ASPH in the MIA PaCa2-empty vector (ASPH ^{low}) and MIA PaCa2-ASPH (ASPH ^{high}) by Western blot. (**C**) Growth curves demonstrating inhibition of tumor progression by SNS-622-DM1 compared to the nonrelevant IgG antibody conjugated DM1. (**D**) Statistical analysis of tumor growth curve.

Drafting of manuscript: H.G., J.W., K.N., X.D.
Statistical analysis: K.N., X.D.
Obtained funding: J.W., S.Z., H.G.
Administrative: R.C.
Technical support: R.C., Z-G. J., M.L.
Material support: S.F., H.G., M.L., J.W., X.B.
Study supervision: H.G., J.W., X.D.

Disclosures

The authors declare the following conflicts of interest: Hossein Ghanbari, Steve Fuller, Zhi-Gang Jiang and Michael S. Lebowitz are full time employees at Sensei Biotherapeutics (previously named as Panacea Pharmaceuticals). The other authors declare no conflict of interest.

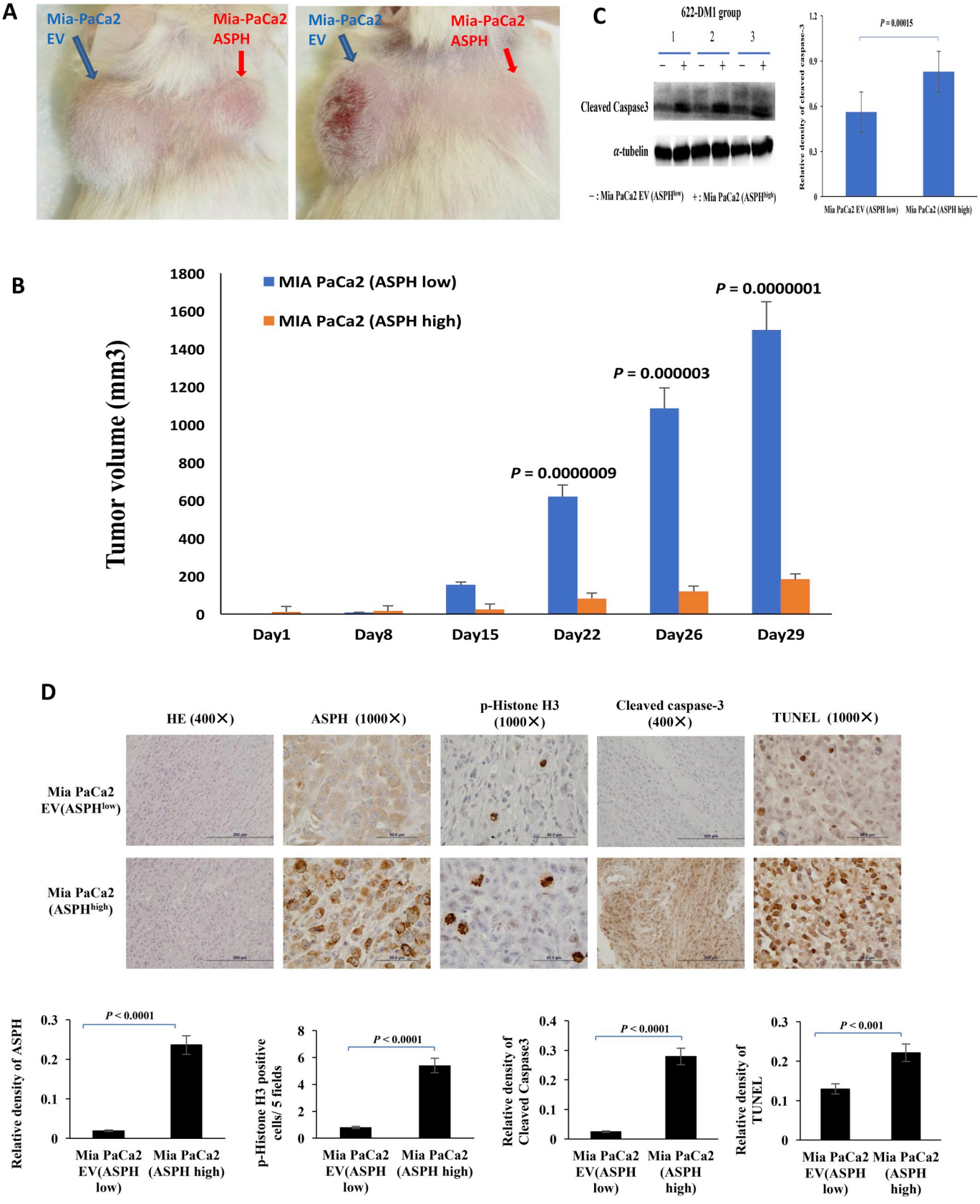

Fig. 7. SNS-622-DM1 blocks tumor growth and promotes apoptosis in a s.c. orthopic murine model. (A) Growth of the parenteral MIA PaCa2 (ASPH ^{low}) compared to MIA PaCa2-ASPH (ASPH ^{high}) cell lines as solid tumors produced on the back of 2 representative NSG mice. **(B)** Note the striking differences in tumor volume generated by the above two cell lines implanted in the same animal over a 29-day period. **(C)** The levels of cleaved caspase 3 as measured by Western blot analysis among three representative tumors treated with SNS-622-DM1. The (−) represents tumors derived from the MIA PaCa2-empty vector (ASPH ^{low}) and (+) represents tumors derived from MIA PaCa2-ASPH (ASPH ^{high}). (D) Analysis of ASPH and p-histone H3 expression levels as well as apoptosis markers of cleaved caspase 3 and the TUNEL assay. There were 12 animals in both Mia PaCa2 EV (ASPH^{low}) and Mia PaCa2 (ASPH^{high}) induced tumors. The ADC SNS-622-DM1 promotes apoptosis as a mechanism for inhibiting tumor growth.

Funding

This work was supported by National Institutes of Health (P30-GM-110759).

Acknowledgments

None.

Appendix A. Supplementary data

Supplementary data to this article can be found online at https://doi.org/10.1016/j.canlet.2019.02.006.

References

[1] I.T. Konstantinidis, A.L. Warshaw, J.N. Allen, L.S. Blaszkowsky, C.F. Castillo, V. Deshpande, T.S. Hong, E.L. Kwak, G.Y. Lauwers, D.P. Ryan, J.A. Wargo, K.D. Lillemoe, C.R. Ferrone, Pancreatic ductal adenocarcinoma: is there a survival difference for R1 resections versus locally advanced unresectable tumors? What is a "true" R0 resection? Ann. Surg. 257 (2013) 731–736.
[2] D.P. Ryan, T.S. Hong, N. Bardeesy, Pancreatic adenocarcinoma, N. Engl. J. Med. 371 (2014) 1039–1049.
[3] N. Diamantis, U. Banerji, Antibody-drug conjugates–an emerging class of cancer treatment, Br. J. Canc. 114 (2016) 362–367.
[4] X. Dong, Q. Lin, A. Aihara, Y. Li, C.K. Huang, W. Chung, Q. Tang, X. Chen, R. Carlson, C. Nadolny, G. Gabriel, M. Olsen, J.R. Wands, Aspartate β-Hydroxylase expression promotes a malignant pancreatic cellular phenotype, Oncotarget 6 (2015) 1231–1248.
[5] Q. Lin, A. Aihara, W. Chung, Y. Li, Z. Huang, X. Chen, S. Weng, R.I. Carlson, J.R. Wands, X. Dong, LRH1 as a driving factor in pancreatic cancer growth, Cancer Lett. 345 (2014) 85–90.
[6] Y.A. Yeung, A.H. Finney, I.A. Koyrakh, M.S. Lebowitz, H.A. Ghanbari, J.R. Wands, K.D. Wittrup, Isolation and characterization of human antibodies targeting human aspartyl (asparaginyl) beta-hydroxylase, Hum. Antib. 16 (2007) 163–176.
[7] N. Ince, S.M. de la Monte, J.R. Wands, Overexpression of human aspartyl (asparaginyl) beta-hydroxylase is associated with malignant transformation, Cancer Res. 60 (2000) 1261–1266.
[8] A.C. Ruifrok, D.A. Johnston, Quantification of histochemical staining by color deconvolution, Anal. Quant. Cytol. Histol. 23 (2001) 291–299.
[9] Y. Iwagami, C.K. Huang, M.J. Olsen, J.M. Thomas, G. Jang, M. Kim, Q. Lin, R.I. Carlson, C.E. Wagner, X. Dong, J.R. Wands, Aspartate β-hydroxylase modulates cellular senescence through glycogen synthase kinase 3β in hepatocellular carcinoma, Hepatology 63 (2016) 1213–1226.
[10] D.M. Euhus, C. Hudd, M.C. LaRegina, F.E. Johnson, Tumor measurement in the nude mouse, J. Surg. Oncol. 31 (1986) 229–234.
[11] M.M. Tomayko, C.P. Reynolds, Determination of subcutaneous tumor size in athymic (nude) mice, Cancer Chemother. Pharmacol. 24 (1989) 148–154.
[12] R.A. de Claro, K. McGinn, V. Kwitkowski, J. Bullock, A. Khandelwal, B. Habtemariam, Y. Ouyang, H. Saber, K. Lee, K. Koti, M. Rothmann, M. Shapiro, F. Borrego, K. Clouse, X.H. Chen, J. Brown, L. Akinsanya, R. Kane, E. Kaminskas, A. Farrell, R. Pazdur, U.S. Food and Drug Administration approval summary: brentuximab vedotin for the treatment of relapsed Hodgkin lymphoma or relapsed systemic anaplastic large-cell lymphoma, Clin. Cancer Res. 18 (2012) 5845–5849.
[13] P.M. LoRusso, D. Weiss, E. Guardino, S. Girish, M.X. Sliwkowski, Trastuzumab emtansine: a unique antibody-drug conjugate in development for human epidermal growth factor receptor 2-positive cancer, Clin. Cancer Res. 17 (2011) 6437–6447.
[14] K. Tsuchikama, Z. An, Antibody-drug Conjugates: Recent Advances in Conjugation and Linker Chemistries, Protein Cell, 2016.
[15] H. Chen, Z. Lin, K.E. Arnst, D.D. Miller, W. Li, Tubulin inhibitor-based antibody-drug conjugates for cancer therapy, Molecules 22 (2017).
[16] P. Polakis, Antibody drug conjugates for cancer therapy, Pharmacol. Rev. 68 (2016) 3–19.
[17] A. Aihara, C.K. Huang, M.J. Olsen, Q. Lin, W. Chung, Q. Tang, X. Dong, J.R. Wands, A cell-surface beta-hydroxylase is a biomarker and therapeutic target for hepatocellular carcinoma, Hepatology 60 (2014) 1302–1313.
[18] C.K. Huang, Y. Iwagami, A. Aihara, W. Chung, S. de la Monte, J.M. Thomas, M. Olsen, R. Carlson, T. Yu, X. Dong, J. Wands, Anti-tumor effects of second generation beta-hydroxylase inhibitors on cholangiocarcinoma development and progression, PLoS One 11 (2016) e0150336.
[19] M.C. Cantarini, S.M. de la Monte, M. Pang, M. Tong, A. D'Errico, F. Trevisani, J.R. Wands, Aspartyl-asparagyl beta hydroxylase over-expression in human hepatoma is linked to activation of insulin-like growth factor and notch signaling mechanisms, Hepatology 44 (2006) 446–457.
[20] Y. Iwagami, C.K. Huang, M.J. Olsen, J.M. Thomas, G. Jang, M. Kim, Q. Lin, R.I. Carlson, C.E. Wagner, X. Dong, J.R. Wands, Aspartate beta-hydroxylase modulates cellular senescence via glycogen synthase kinase 3beta in hepatocellular carcinoma, Hepatology 63 (4) (2016) 1213–1226.
[21] T. Noda, M. Shimoda, V. Ortiz, A.E. Sirica, J.R. Wands, Immunization with aspartate-beta-hydroxylase-loaded dendritic cells produces antitumor effects in a rat model of intrahepatic cholangiocarcinoma, Hepatology 55 (2012) 86–97.
[22] M. Shimoda, Y. Tomimaru, K.P. Charpentier, H. Safran, R.I. Carlson, J. Wands, Tumor progression-related transmembrane protein aspartate-beta-hydroxylase is a target for immunotherapy of hepatocellular carcinoma, J. Hepatol. 56 (5) (2012) 1129–1135.
[23] T. Maeda, K. Taguchi, S. Aishima, M. Shimada, D. Hintz, N. Larusso, G. Gores, M. Tsuneyoshi, K. Sugimachi, J.R. Wands, S.M. de la Monte, Clinicopathological correlates of aspartyl (asparaginyl) beta-hydroxylase over-expression in cholangiocarcinoma, Cancer Detect. Prev. 28 (2004) 313–318.
[24] K. Wang, J. Liu, Z.L. Yan, J. Li, L.H. Shi, W.M. Cong, Y. Xia, Q.F. Zou, T. Xi, F. Shen, H.Y. Wang, M.C. Wu, Overexpression of aspartyl-(asparaginyl)-beta-hydroxylase in hepatocellular carcinoma is associated with worse surgical outcome, Hepatology 52 (2010) 164–173.
[25] K. Almhanna, D. Wright, T.M. Mercade, J.L. Van Laethem, A.C. Gracian, C. Guillen-Ponce, J. Faris, C.M. Lopez, R.A. Hubner, J. Bendell, A. Bols, J. Feliu, N. Starling, P. Enzinger, D. Mahalingham, W. Messersmith, H. Yang, A. Fasanmade, H. Danaee, T. Kalebic, A phase II study of antibody-drug conjugate, TAK-264 (MLN0264) in previously treated patients with advanced or metastatic pancreatic adenocarcinoma expressing guanylyl cyclase C, Invest. N. Drugs 35 (2017) 634–641.
[26] K. Almhanna, M.L. Miron, D. Wright, A.C. Gracian, R.A. Hubner, J.L. Van Laethem, C.M. Lopez, M. Alsina, F.L. Munoz, J. Bendell, I. Firdaus, W. Messersmith, Z. Ye, A.A. Fasanmade, H. Danaee, T. Kalebic, Phase II study of the antibody-drug conjugate TAK-264 (MLN0264) in patients with metastatic or recurrent adenocarcinoma of the stomach or gastroesophageal junction expressing guanylyl cyclase C, Invest. N. Drugs 35 (2017) 235–241.
[27] M. Mattie, A. Raitano, K. Morrison, Z. An, L. Capo, A. Verlinsky, M. Leavitt, J. Ou, R. Nadell, H. Aviña, C. Guevara, F. Malik, R. Moser, S. Duniho, J. Coleman, Y. Li, D.S. Pereira, F. Doñate, I.B. Joseph, P. Challita-Eid, D. Benjamin, D.R. Stover, The discovery and preclinical development of ASG-5ME, an antibody-drug conjugate targeting SLC44A4-positive epithelial tumors including pancreatic and prostate cancer, Mol. Canc. Therapeut. 15 (2016) 2679–2687.
[28] N.H. Stoecklein, A.M. Luebke, A. Erbersdobler, W.T. Knoefel, W. Schraut, P.E. Verde, F. Stern, P. Scheunemann, M. Peiper, C.F. Eisenberger, J.R. Izbicki, C.A. Klein, S.B. Hosch, Copy number of chromosome 17 but not HER2 amplification predicts clinical outcome of patients with pancreatic ductal adenocarcinoma, J. Clin. Oncol. 22 (2004) 4737–4745.
[29] M. Barok, M. Tanner, K. Koninki, J. Isola, Trastuzumab-DM1 is highly effective in preclinical models of HER2-positive gastric cancer, Cancer Lett. 306 (2011) 171–179.
[30] M. Apicella, S. Corso, S. Giordano, Targeted therapies for gastric cancer: failures and hopes from clinical trials, Oncotarget 8 (2017) 57654–57669.
[31] A. Sartore-Bianchi, L. Trusolino, C. Martino, K. Bencardino, S. Lonardi, F. Bergamo, V. Zagonel, F. Leone, I. Depetris, E. Martinelli, T. Troiani, F. Ciardiello, P. Racca, A. Bertotti, G. Siravegna, V. Torri, A. Amatu, S. Ghezzi, G. Marrapese, L. Palmeri, E. Valtorta, A. Cassingena, C. Lauricella, A. Vanzulli, D. Regge, S. Veronese, P.M. Comoglio, A. Bardelli, S. Marsoni, S. Siena, Dual-targeted therapy with trastuzumab and lapatinib in treatment-refractory, KRAS codon 12/13 wild-type, HER2-positive metastatic colorectal cancer (HERACLES): a proof-of-concept, multicentre, open-label, phase 2 trial, Lancet Oncol. 17 (2016) 738–746.
[32] Y. Yamanaka, H. Friess, M.S. Kobrin, M. Buchler, J. Kunz, H.G. Beger, M. Korc, Overexpression of HER2/neu oncogene in human pancreatic carcinoma, Hum. Pathol. 24 (1993) 1127–1134.
[33] H. Safran, M. Steinhoff, S. Mangray, R. Rathore, T.C. King, L. Chai, K. Berzein, T. Moore, D. Iannitti, P. Reiss, T. Pasquariello, P. Akerman, D. Quirk, R. Mass, L. Goldstein, U. Tantravahi, Overexpression of the HER-2/neu oncogene in pancreatic adenocarcinoma, Am. J. Clin. Oncol. 24 (2001) 496–499.
[34] S. Artavanis-Tsakonas, M.D. Rand, R.J. Lake, Notch signaling: cell fate control and signal integration in development, Science 284 (1999) 770–776.
[35] L. Lavaissiere, S. Jia, M. Nishiyama, S. de la Monte, A.M. Stern, J.R. Wands, P.A. Friedman, Overexpression of human aspartyl(asparaginyl)beta-hydroxylase in hepatocellular carcinoma and cholangiocarcinoma, J. Clin. Invest. 98 (1996) 1313–1323.
[36] T. Maeda, P. Sepe, S. Lahousse, S. Tamaki, M. Enjoji, J.R. Wands, S.M. de la Monte, Antisense oligodeoxynucleotides directed against aspartyl (asparaginyl) beta-hydroxylase suppress migration of cholangiocarcinoma cells, J. Hepatol. 38 (2003) 615–622.
[37] P.S. Sepe, S.A. Lahousse, B. Gemelli, H. Chang, T. Maeda, J.R. Wands, S.M. de la Monte, Role of the aspartyl-asparaginyl-beta-hydroxylase gene in neuroblastoma cell motility, Laboratory Investigation; a Journal of Technical Methods and Pathology, vol. 82, 2002, pp. 881–891.
[38] M. Luu, E. Sabo, S.M. de la Monte, W. Greaves, J. Wang, R. Tavares, L. Simao, J.R. Wands, M.B. Resnick, L. Wang, Prognostic value of aspartyl (asparaginyl)-beta-hydroxylase/humbug expression in non-small cell lung carcinoma, Hum. Pathol. 40 (2009) 639–644.
[39] J. Wang, S.M. de la Monte, E. Sabo, S. Kethu, R. Tavares, M. Branda, L. Simao, J.R. Wands, M.B. Resnick, Prognostic value of humbug gene overexpression in stage II colon cancer, Hum. Pathol. 38 (2007) 17–25.
[40] W. Chung, M. Kim, S. de la Monte, L. Longato, R. Carlson, B.L. Slagle, X. Dong, J.R. Wands, Activation of signal transduction pathways during hepatic oncogenesis, Cancer Lett. 370 (2016) 1–9.